frontiers | Frontiers in Environmental Chemistry

TYPE Original Research
PUBLISHED 19 March 2025
DOI 10.3389/fenvc.2025.1559968

OPEN ACCESS

EDITED BY
Robert Peter Mason,
University of Connecticut, United States

REVIEWED BY
Hongwei Liu,
Sun Yat-sen University, China
Hanbing Li,
Nanjing University, China

*CORRESPONDENCE
Mathilde Monperrus,
mathilde.monperrus@univ-pau.fr

RECEIVED 13 January 2025
ACCEPTED 05 March 2025
PUBLISHED 19 March 2025

CITATION
Bakour I, Isaure M-P, Barrouilhet S, Goñi-Urriza M and Monperrus M (2025) Mercury interaction with S-containing molecules: implications for methylation and demethylation processes in a sulfate reducing bacteria.
Front. Environ. Chem. 6:1559968.
doi: 10.3389/fenvc.2025.1559968

Mercury interaction with S-containing molecules: implications for methylation and demethylation processes in a sulfate reducing bacteria

Ikram Bakour[1], Marie-Pierre Isaure[2], Sophie Barrouilhet[2], Marisol Goñi-Urriza[2] and Mathilde Monperrus[1]*

[1]Universite de Pau et des Pays de l'Adour, E2S UPPA, CNRS, IPREM UMR 5254, Anglet, France, [2]Universite de Pau et des Pays de l'Adour, E2S UPPA, CNRS, IPREM UMR 5254, Pau, France

Mercury methylation by anaerobic microorganisms, including sulfate-reducing bacteria (SRB), is a key process in the production of neurotoxic methylmercury (MeHg). The chemical speciation of mercury (Hg) strongly influences its bioavailability as well as its potential for methylation and demethylation, with sulfur-containing ligands playing a critical role in these processes. In this study, we used isotopically enriched mercury species (^{199}Hg(II), Me^{202}Hg) to investigate how molecular speciation of mercury affects both methylation and demethylation processes by the sulfate-reducer *Pseudodesulfovibrio hydrargyri* BerOc1. Experimental assays were carried out: (i) without external addition of S-ligands, (ii) with the addition of increasing concentrations of exogenous cysteine (Cys) (0.01, 0.1, and 0.5 mM), or (iii) with the addition of exogenous sulfide (0.1 mM). We showed that the highest methylation rate (K_{meth}) was obtained without the external addition of S-ligands, whereas the addition of Cys or sulfide decreased Hg methylation regardless of Cys concentration. By quantitatively determining Hg(II) speciation in extracellular fractions, we demonstrated that Hg(II) was mostly present in the form of $Hg(Cys)_2$, when Cys was added. However, metabolically sulfide production from Cys degradation shifted the chemical speciation of Hg(II) from $Hg(Cys)_2$ to a more insoluble fraction ($HgS_{(S)}$). In the assay without externally added ligands (Cys or sulfide), speciation models were generated by taking in account the metabolically produced thiols. These models established the predominance of Hg(II) complexes with a mixed ligation involving biosynthesized thiols, OH^-, and Cl^- ions. Our results suggest that these complexes with lower thermodynamic stabilities enhance the MeHg formation rate compared to the more stable $Hg(Cys)_2$ or $HgS_{(s)}$ species. Unlike Hg(II) methylation, the addition of S-ligands did not affect the rates of demethylation (K_{demeth}) of MeHg, even though it caused a shift in the chemical speciation of MeHg (from MeHgCl to MeHgCys and MeHgSH). These findings contribute to our understanding of the potential role of specific S-ligands and chemical speciation in governing the environmental fate and toxicity of mercury.

KEYWORDS

speciation, bioavailability, thiols, sulfides, Hg transformations, pure strain culture, isotopic tracers, hyphenated mass spectrometry techniques

1 Introduction

The methylation of inorganic mercury [Hg(II)] by diverse anaerobic microorganisms, including sulfate reducers (SRB), iron reducers (IRB), and methanogens is driven by the *hgcAB* gene cluster. This process is a crucial step in the production of MeHg (Gilmour et al., 2013; Parks et al., 2013; Gilmour et al., 2018; Bravo et al., 2018; Goñi-Urriza et al., 2020). Microbial methylation occurs primarily in anoxic environments such as sediments and soils (Compeau and Bartha, 1985), where Hg speciation is expected to be regulated by thiol-containing ligands present in natural organic matter (NOM) or sulfides (Liem-Nguyen et al., 2017a). However, while sulfur-containing ligands exhibit the highest affinity for Hg compared to other ligands (Liem-Nguyen et al., 2017a; Liem-Nguyen et al., 2017b), our understanding of the mechanism by which these S-ligands affect the speciation and bioavailability of Hg(II) remains limited.

Experimental addition of exogenous S-ligands has been one approach to elucidate the potential impact of complexing ligands present in the environment. In summary, the addition of approximately 1–10 μM of specific low molecular mass thiols (LMM-RSH), particularly Cysteine (Cys), has been demonstrated to significantly increase the rates of methylation of Hg(II) in methylating strains such as the iron reducer *Geobacter sulfurreducens* (Schaefer and Morel, 2009; Schaefer et al., 2011; Lin et al., 2015; Lu et al., 2016), the sulfate reducer *Desulfovibrio desulfuricans* ND132 (Graham et al., 2012a), and non-methylating strains like *Escherichia coli* (Ndu et al., 2012; Thomas et al., 2014). Other thiols such as glutathione (GSH) or penicillamine (PEN) were reported to either increase or suppress Hg methylation depending on bacterial strain (Schaefer et al., 2011). This suggests that the concentration of thiols and their specific binding to Hg in the extracellular environment can regulate Hg methylation, and it is also strain-dependent. The increase in Hg(II) methylation in the presence of micromolar thiol addition has been generally attributed to a change in the chemical speciation of Hg(II) from $HgCl_nOH_{(1-n)}$ species to the predominance of Hg $(LMM\text{-}RS)_2$ complexes (Schaefer and Morel, 2009; Lin et al., 2015), which were hypothesized to be more bioavailable to the model strains studied.

In addition to the role of thiols, the implication of sulfide, another Hg complexing ligand has likewise been investigated. Optimum exogenous addition of sulfides up to 500 μM and 200 μM enhanced Hg (II) methylation potential in the sulfate reducers *Pseudodesulfovibrio hydrargyri* BerOc1 (40%) (Barrouilhet et al., 2022), and ND132 (from ~2 to >20-fold) (Graham et al., 2013), respectively. Maximal methylation was also observed at sulfide concentrations below 100 μM for three strains of methanogenic archaea (Gilmour et al., 2018). It has been suggested that the enhancement in Hg methylation was the consequence of the formation of nanoscale β-HgS(s) particles (Graham et al., 2013; Deonarine and Hsu-Kim, 2009; Gerbig et al., 2011; Graham et al., 2012b; Zhang et al., 2012; Pham et al., 2014).

The addition of exogenous S-ligands in excess (as discussed above) has been one approach for investigating their roles in Hg(II) methylation. However, thiols and/or sulfide may also be metabolically produced and exported by microorganisms (Barrouilhet et al., 2022; Hand and Honek, 2005; Adediran et al., 2019; Thomas et al., 2019; Bakour et al., 2023; Gutensohn et al., 2023) at concentrations that are sufficient to control Hg speciation and bioavailability (Adediran et al., 2019). Several microorganisms have demonstrated the ability to degrade Cys and produce biogenic sulfide. The degradation of Cys to sulfides has been observed in *E. coli* strains (Awano et al., 2005; Shimada et al., 2016; Thomas and Gaillard, 2017; Thomas et al., 2019; Stenzler et al., 2022), *Desulfovibrio* species (Graham et al., 2012a), including the model strain *P. hydrargyri* BerOc1 (Barrouilhet et al., 2022; Bakour et al., 2023). Consequently, previous studies with exogenous Cys addition are likely to involve a mixture of Hg(II)-thiol and Hg(II)-sulfide species, introducing uncertainties in the interpretation of the results. Moreover, for the methylating strains that are both able to methylate and demethylate Hg, these S-ligands may control both processes (methylation and demethylation) and impact the final net production of MeHg. The implications of S-ligands in the demethylation process are still unclear. In this study, we investigated the role of S-ligands (Cys and sulfide), metabolically produced and/or exogenously present in the external environment, in controlling Hg molecular speciation and transformations (methylation and demethylation) in the sulfate-reducing bacterium *P. hydrargyri* BerOc1, a well-established SRB model capable of methylating Hg(II) and demethylating MeHg (Barrouilhet et al., 2022; Ranchou-Peyruse et al., 2009; Pedrero et al., 2012; Goñi-Urriza et al., 2015; Isaure et al., 2020). We utilized isotopically enriched Hg species ($^{199}Hg(II)$, $Me^{202}Hg$) to simultaneously track Hg species and transformations, which could lead to a more precise interpretation of the impact of S-ligands on these processes. Experiments were conducted (i) without the external addition of S-ligands, to investigate the effect of metabolically produced ones (ii) with increasing concentrations of Cys, or (iii) with the addition of sulfide. Subsequently, the potentials and rates of Hg methylation and demethylation, partitioning of Hg species, molecular speciation of Hg(II) and MeHg, microbial Cys degradation, and production of sulfide and other thiols were investigated in BerOc1. By quantifying and considering the microbially produced thiol compounds, we conducted experiments at environmentally relevant concentrations of such compounds and generated refined speciation models for Hg(II) and MeHg in assay media.

2 Materials and methods

2.1 Microbial culture conditions

Pseudodesulfovibrio hydrargyri BerOc1, a sulfate-reducing strain isolated from Berre Lagoon sediment, is a well-known SRB model able to both methylate inorganic mercury Hg(II) and to demethylate methylmercury (MeHg) (Ranchou-Peyruse et al., 2009; Pedrero et al., 2012; Goñi-Urriza et al., 2015; Isaure et al., 2020; Barrouilhet et al., 2022). BerOc1 was grown anaerobically in the dark at 37 °C and pH 7.0–7.1 in a multipurpose medium (Widdel et al., 1992) under fumarate respiration with 40 mM pyruvate as the electron donor and 40 mM fumarate as the electron acceptor (Supplementary Text S2). Cells were harvested in the early stationary phase (optical density $OD_{600\ nm}$ at ~0.4–0.5). The growing cell cultures were carefully transferred into 250-mL

PTFE centrifuge flasks under anoxic conditions and centrifuged (at 8,000 g, 15 min, 25°C). Cell pellets were collected, pooled, and sequentially washed three times with mineral base medium. The final washed cells were gently homogenized in 50 mL of fresh anoxic medium.

For each experimental condition, 500 mL of multipurpose medium containing 1 mM pyruvate and 1 mM fumarate was inoculated with 8 mL aliquot of washed cell suspensions to a final optical density of 0.2, equivalent to final assay with ~10^8 cells. mL^{-1}, a cells density typical of pure culture experiments with *P. hydrargyri* BerOc1 (Pedrero et al., 2012; Isaure et al., 2020). For conditions with external S-ligand addition, Cys (0.01, 0.1, or 0.5 mM) or sulfide (0.1 mM) were added and allowed to equilibrate for 30 min before the addition of Hg. All stock solutions of Cys (≥99%, Acros Organics) and Na_2S, $9H_2O$ (98%, Alfa Aesar) were prepared in deoxygenated Milli-Q water (>18 MΩ cm) inside a glove box amended with N_2.

2.2 Simultaneous Hg methylation and demethylation kinetic assays

All methylation assays were conducted in autoclaved penicillin flasks prewashed by ultrasonication in 10% HNO_3 and HCl baths and rinsed with ultrapure Milli-Q water. For Hg exposure, 50 µL of 0.5 µM of $^{199}HgCl_2$ enriched standard solution (ISC science), and 50 µL of 0.05 µM of $Me^{202}Hg$ chloride (LGC standards) were spiked into the cultures. The cultures under each condition were distributed into penicillin flasks and incubated at 37°C for 0, 4 h, 8 h, 20 h, 28 h, or 48 h in triplicates. Controls with inactive bacteria were performed with heated cells (80°C for 1 h) exposed to 0.05 µM of ^{199}Hg(II), 0.05 µM of $Me^{202}Hg$, either without the addition of S-ligands or with 0.1 mM Cys or 0.1 mM sulfide.

2.3 Hg(II) and MeHg partitioning and analysis

At the end of Hg exposure, an aliquot of 0.5 mL of the cell culture (bulk fraction) was sampled and digested in 50% (v/v) of 6 N nitric acid (HNO_3) for Hg(II) and MeHg analysis. 1 mL of the remaining cell culture was then filtered at 0.2 µm (PVDF filter), and 0.5 mL was collected in 50% (v/v) 6 N HNO_3 (extracellular fraction). The samples were stored at 4°C until further analysis. Isotopically enriched Hg(II) and MeHg concentrations were measured using capillary gas chromatography (GC TriPlus™ RSH™, Thermo Scientific) connected to an inductively coupled plasma mass spectrometer (ICPMS, X2-series, Thermo Electron) (Pedrero et al., 2012; Bridou et al., 2011). Quantification of isotopically enriched Hg(II) and MeHg was carried out by reverse isotope dilution analysis. To summarize, a known amount of fractions (bulk or extracellular) was buffered at pH 3.9 with a 0.1 M acetic acid/acetate buffer before being spiked with a known amount of isotopically enriched Hg species (^{198}Hg(II) and $Me^{201}Hg$) as internal standards. Both Hg(II) and MeHg were ethylated with 5% (v/v) $NaBEt_4$ and extracted with isooctane by vigorous shaking for 20 min. The organic phase containing the Hg species was collected and analyzed using GC-ICPMS. The experimental data were mathematically processed by isotope pattern deconvolution approaches previously developed (Rodríguez-González et al., 2007). This technique allows the quantification of both Hg species concentrations and transformation factors (i.e., methylation and demethylation) affecting the two isotopic tracers during the analytical procedure. The analytical setup and methodology of GC-ICPMS for mercury speciation analysis are described in detail elsewhere (Ranchou-Peyruse et al., 2009; Pedrero et al., 2012).

Hg methylation potential and Hg species partitioning were determined in the same batch culture. Methylation potentials were calculated in bulk cultures by dividing the MeHg concentration produced (T_{final-} $T_{initial,}$ T_f-T_i) by the total Hg concentration measured at T_i. The partitioning of each Hg species (Hg(II) and MeHg) in the extracellular fractions was calculated by dividing the Hg species concentrations in the supernatant by the Hg species concentrations in the bulk fraction ×100. The percentage of Hg species in the pellet (i.e., cell-associated fraction including sorbed and intracellular Hg and particles in the medium) was determined by subtracting the percentage of Hg species in the supernatant fraction from 100%.

Specific methylation and demethylation rate constants (K_{meth} and K_{demeth}) were calculated for time series experiments using a first-order reversible reaction kinetic model. The mathematical steps for assessing the rate constants were discussed in detail by (Rodrı´guez Martı´n-Doimeadios et al., 2004). Assuming a pseudo-first-order reversible reaction, the net MeHg formation can be expressed as follows:

$$\frac{d[MeHg]}{dt} = K_{meth}\,[Hg(II)] - K_{demeth}\,[MeHg] \qquad (1)$$

By applying the kinetic model, it was possible to obtain both rate constants from species concentrations obtained from time-series experiments using the BoxLucas1 fitting model (Origin Lab software).

With the assumption that $[Me^{199}Hg]_0 = 0$ at the onset of the reaction, Equation 1 can thus be integrated to obtain $[Me^{199}Hg]$ as a function of time.

$$\frac{[Me^{199}Hg]}{[^{199}Hg\,(II)]_o} = \frac{K_{meth}}{K_{meth} + K_{demeth}}\left(1 - e^{-(K_{meth}+K_{demeth})t}\right) \qquad (2)$$

The $[Me^{199}Hg]/[^{199}Hg\ (II)]_0$ ratios were then plotted against incubation time (in hours) using Origin 6.1 software. The Box Lucas one exponential fitting model was used to resolve Equation 2 and calculate the methylation (K_m) and demethylation (K_d) rate constants.

2.4 Hg molecular speciation analysis and modelling

The concentrations of $^{199}Hg(Cys)_2$, $Me^{199}Hg$-Cys, and $Me^{202}Hg$-Cys complexes were determined using an Acquity ultra performance liquid chromatography (UPLC) system (Waters, Milford, MA) equipped with a binary solvent pump and a cooled autosampler connected to a Xevo TQ mass spectrometer (MS). The complexes were separated using an Acquity UPLC HSS T3 C18 column (2.1 × 50 mm, 1.8 µm, Waters) with a matching Vanguard precolumn. Aliquots of 10 µL were injected at 0.35 $mL{\cdot}min^{-1}$ for the mobile phase consisting of 0.1% formic acid in water (A) and 0.1% formic acid in MeOH (B). We applied offline solid-phase extraction (SPE) using

a mixed-mode reversed-phase ion-exchanger sorbent (Oasis Mcx 3 Cc Vac Cartridge, 60 mg, 30 µm particle Size) for selective preconcentration of the Hg complexes with an eluting solvent consisting of MeOH/water (60:40 v/v). Detection was performed in both positive and negative electrospray ionization modes (ESI). The method for MeHg complexes was adapted from Liem-Nguyen et al. (Liem-Nguyen et al., 2020), incorporating an offline SPE preconcentration. The limits of detection in this study were 8 nM for MeHg-Cys and 4 nM for $Hg(Cys)_2$. The general operating conditions of the instrument are listed in Supplementary Table S1. The complexes were determined in extracellular fractions of BerOc1 at each kinetic point after filtration through 0.2 µm syringe filters.

To investigate the other possible Hg species that can be formed in *P. hydrargyri* BerOc1 culture assays, we used Visual Minteq software to perform thermodynamic modeling. The ranges of Log K and possible reactions were adopted from Compeau and Bartha (1985). Our thermodynamic calculations incorporated the total sulfide, cysteine, metabolically produced thiols, and total Hg and MeHg concentrations measured in the exposure medium. The complete speciation model is presented in Supplementary Table S2.

2.5 Sulfide and (LMM-RSH) thiols analysis

Sulfide was measured in the assay medium using a sulfide-reactive coumarin fluorescent probe, known as α, β-unsaturated ethanoylcoumarin (DHC) (Yang et al., 2019), after adapting the method for sulfide detection in *P. hydrargyri* BerOc1 cultures assays (Bakour et al., 2023). The detection limit using this approach was 20 nM. For analysis, 1 mL of the bulk fraction was collected at each kinetic point and analyzed using the DHC probe.

The concentrations of specific LMM-RSH thiol compounds including Cys, 2-Mercaptoethanesulfonic acid (SULF), PEN, N-acetyl-L-cysteine (NacCys), mercaptosuccinic acid (SUC), 2-Mercaptopropionic acid (2-MPA), GSH, cysteamine (Cyst),1-Thiolglycerol (Glyc), mercaptoacetic acid (Mac), N-acetyl-D-penicillamine (NacPen), L-homocysteine (HCys), γ-L-glutamyl-L-cysteine (γ-Glu-Cys), and cysteine-glycine (Cys-Gly) were determined according to (Liem-Nguyen et al., 2015), after adapting the method for UPLC-ESI-MS instrument and using offline SPE preconcentration (details cited above and in Supplementary Table S1). We applied offline SPE using an oasis hydrophilic-lipophilic balanced reversed-phase sorbent (HLB: 3 cc Vac Cartridge, 60 mg, 30 µm) for the selective preconcentration of thiol compounds with an eluting solvent consisting of MeOH/water (10:90 v/v). The limit of detection was 3–6 nM for all the LMM thiols investigated. The compounds were determined in extracellular fractions of BerOc1 at each kinetic point after filtration through 0.2 µm syringe filters.

3 Results and discussion

3.1 Simultaneous methylation and demethylation in the absence and presence of externally added S- ligands

We used isotopically enriched Hg species to conduct experimental assays with and without the addition of S-containing ligands (Cys and sulfide) to assess their roles in Hg transformations. The availability of isotopically enriched Hg species for the transformation processes was evaluated. The concentrations at the end of the incubation period were always recovered for both $^{199}Hg(II)$ and $Me^{202}Hg$ (~106 and 90%, respectively). A few $Me^{202}Hg$ losses were observed, which could be attributed to either sorption to the bottle walls or to particles in the culture medium. The production of $Me^{199}Hg$ resulting from $^{199}Hg(II)$ methylation increased exponentially within the first few hours and reached a steady state after 28 h of incubation (Figure 1C). The transformation rate constants obtained using the kinetic model approaches applied to Hg species showed a high methylation rate (K_{meth}) in the experiments without the external addition of S-ligands ($2.1 \pm 0.2 \times 10^{-10}$ mL cell^{-1} h^{-1}) (Figure 1A). The addition of exogenous Cys decreased the methylation rate and no significant difference was observed in K_{meth} with increasing Cys concentrations from 0.01 to 0.5 mM (~1.1×10^{-10} mL cell^{-1} h^{-1}, $p > 0.05$, Kruskal–Wallis). The addition of 0.1 mM sulfide resulted in the lowest methylation rate ($0.4 \pm 0.2 \times 10^{-10}$ mL cell^{-1} h^{-1}) (Figure 1A). In another study, higher methylation potentials were observed when BerOc1 was exposed to 0.1 mM sulfide compared to 0.1 mM Cys (Barrouilhet et al., 2022). Here, we demonstrated a higher methylation potential upon the addition of 0.1 mM Cys compared to 0.1 mM of sulfide. However, it is important to note that, despite using the same strain, BerOc1, the experimental conditions varied. The previous study investigated BerOc1 under growth conditions, while in this study, we used resting cell conditions. Additionally, the concentrations of Hg(II) were not identical, leading to variations in the Hg(II)/Cys or Hg(II)/sulfide ratios in the exposure medium.

Unlike Hg(II) methylation, the results showed that the addition of Cys or sulfide had no effect on the MeHg demethylation rates by *P. hydrargyri* BerOc1. No significant difference has been found ($p > 0.05$, Kruskal-Wallis) (Figure 1A). The production of $^{202}Hg(II)$ resulting from $Me^{202}Hg$ degradation increased exponentially within the first few hours and reached a steady state after 28 h of incubation (Figure 1D). In the absence of sulfur ligands, the concentration of $^{202}Hg(II)$ decreased after 28 h (Figure 1D). This decrease is attributed to an enhanced methylation of Hg(II) under these conditions, accounting for the observed reduction.

The demethylation rates (K_{demeth}) was 4–16 times higher than methylation rates (K_{meth}), as previously reported for BerOc1 (Perrot et al., 2015), demonstrating that demethylation efficiency is greater than that of methylation. This ratio decreased with the addition of Cys or sulfide, highlighting the significant role of these S-complexing ligands in regulating the net MeHg production by bacterial cells. This decrease is attributed to the decrease in Hg(II) methylation observed in the presence of S-ligands, as demethylation was not affected.

To go deeper into the implications of S-ligands (Cys and sulfide) in Hg speciation and methylation/demethylation, we conducted further investigations into the molecular speciation and partitioning of Hg, as well as the metabolism of S-compounds.

3.2 Hg(II) and MeHg species partitioning

We investigated Hg species partitioning between the extracellular and cell-associated/particulate (i.e., cell-sorbed,

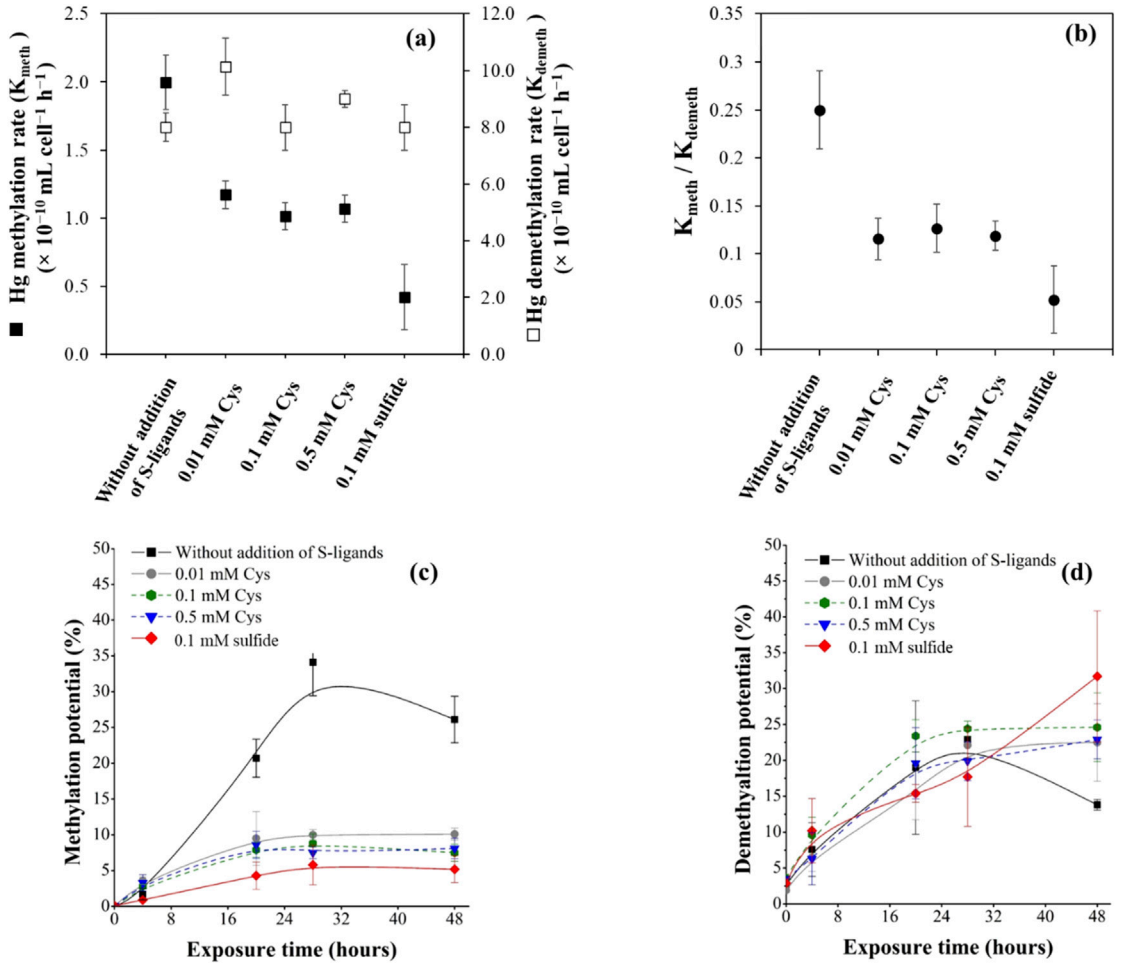

FIGURE 1
(a) Hg methylation rate K_{meth} (black squares) and MeHg demethylation rate K_{demeth} (white squares) determined for pure strain cultures of *P. hydrargyri* BerOc1 tested under different conditions (without external addition of S-ligands, with 0.01, 0.1, and 0.5 mM Cys, or with 0.1 mM of sulfide), after incubation with 0.5 μM ^{199}Hg(II) and 0.05 μM of Me^{202}Hg for 48 h. **(b)** Ratio of K_{meth}/K_{demeth} for the different conditions. **(c)** Hg methylation potentials (% of total recovered ^{199}Hg(II) converted to Me^{199}Hg) **(d)** MeHg demethylation potentials (% of total recovered Me^{202}Hg converted to ^{202}Hg(II)). Error bars represent the standard deviations of three independent replicates.

intracellular and particulate) fractions in BerOc1 incubated under different conditions (Figure 2; Figure 3).

3.2.1 Hg(II) partitioning

^{199}Hg(II) added to the culture and ^{202}Hg(II) formed by biotic demethylation showed dissimilar partitioning. In general, ^{199}Hg(II) added to the culture was in the extracellular fraction, but also associated with cells/particulate fractions (20%–60%) (Figure 2), as previously observed for BerOc1(Pedrero et al., 2012; Barrouilhet et al., 2022). Conversely, only ~20% of the ^{202}Hg(II) resulting from demethylation is associated with cells, while the major fraction is found in the extracellular medium (Supplementary Figure S1).

Varying concentrations of Cys (0.01, 0.1, and 0.5 mM) or sulfide (0.1 mM) do not influence the distribution of ^{202}Hg(II) produced through biotic demethylation (Supplementary Figure S1). Nevertheless, for ^{199}Hg(II) introduced to the culture, the cellular/particulate fraction association increased with rising Cys levels after 20 h of exposure (Figures 2B–D). When 0.5 mM Cys was added, BerOc1 cells showed approximately 80% of Hg(II) associated with cellular/particulate fractions at 48 h (Figure 2D). In the case of sulfide addition, about 60% of ^{199}Hg(II) was primarily associated with cellular/particulate fractions from the initial hours of exposure (Figure 2E).

3.2.2 MeHg partitioning

The distribution of Me^{202}Hg introduced to the culture and Me^{199}Hg produced through biotic processes was found to be similar, with approximately 95% located in the extracellular fraction (Figure 3; Supplementary Figure S2), confirming previous findings. The formed MeHg was immediately exported. Earlier research noted no significant lags in the export of synthesized Hg(II) and MeHg, suggesting that the excreted Hg had minimal affinity or low selectivity for cell surface receptors and transporters (Schaefer and Morel, 2009; Gilmour et al., 2011; Schaefer et al., 2011; Graham et al., 2012a). Introducing increasing concentrations of Cys (0.01, 0.1, and

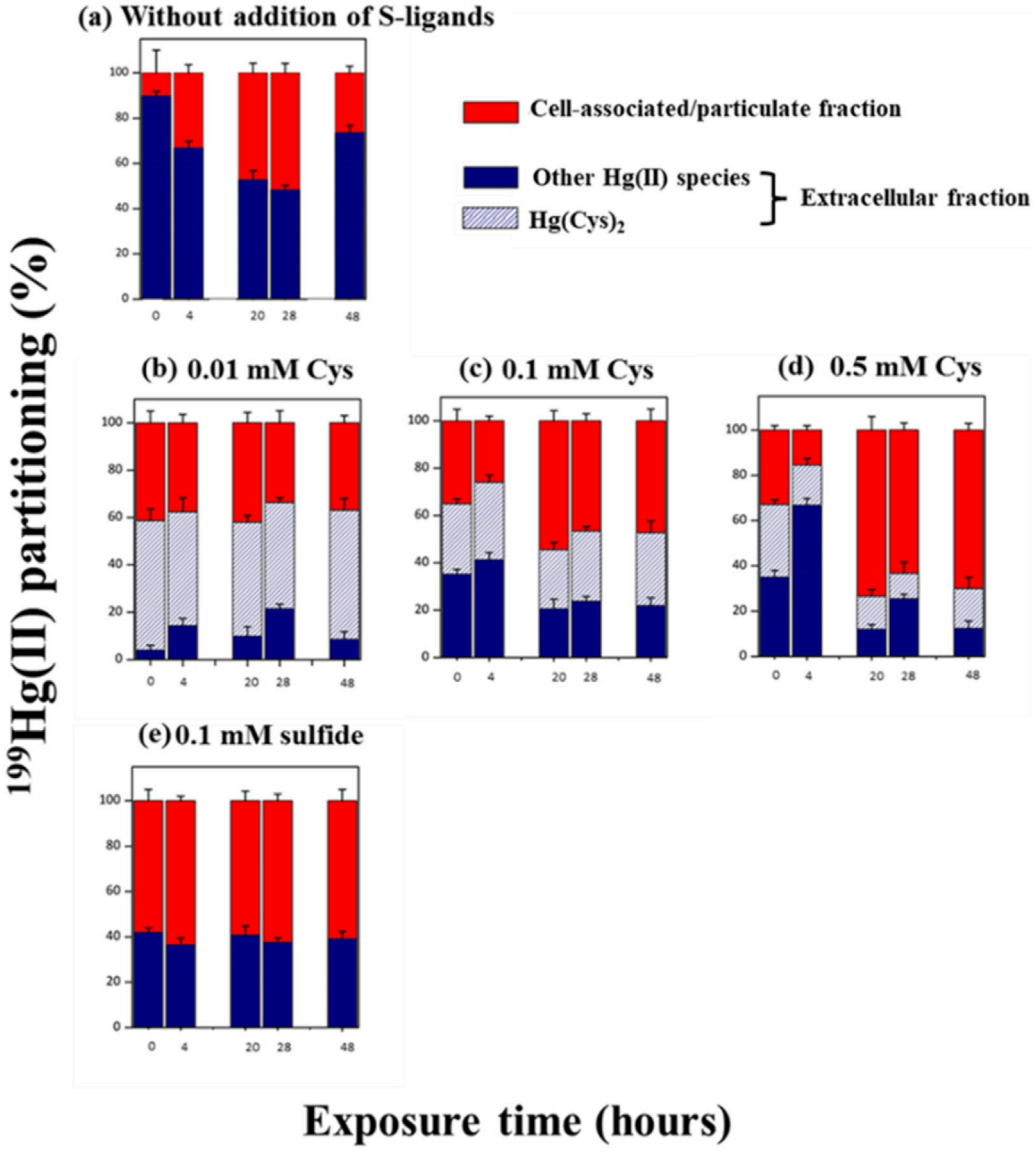

FIGURE 2
Partitioning (%) of added ^{199}Hg(II) between extracellular (blue), the % of Hg(Cys)2 complex detected in the extracellular fraction (blue dash) and cell associated/particulate (red) fractions at the time = 0, 4, 20, 28 and 48 h during exposure to 0.5 μM of ^{199}Hg(II) and 0.05 μM of Me^{202}Hg. **(a)** Experimental without addition of external S-ligands **(b)** with the addition of 0.01 mM of Cys **(c)** 0.1 mM Cys **(d)** 0.5 mM Cys **(e)** 0.1 mM of sulfide. The percentage was calculated by considering the Hg concentration in the three studied fractions. The same culture batches were used to determine the Hg species in the bulk and extracellular fractions for each kinetics. After sampling for Hg species determination using GCICPMS (bulk + supernatant), cultures were filtered (0.2 μm), and the molecular speciation of Hg(II) was measured in the extracellular fraction using LCMSMS. Error bars represent the averages from three independent experiments, and the error bars are ±1 S.D.

0.5 mM) or sulfide (0.1 mM) did not substantially impact the partitioning of either added Me^{202}Hg or biotically methylated Me^{199}Hg (Figure 3; Supplementary Figure S2). Nevertheless, it was observed that in the experiment with 0.1 mM sulfide addition, a higher proportion of Me^{199}Hg (100%) was exported to the extracellular fraction compared to other conditions (~80%) (Supplementary Figure S2). For BerOc1, a strong positive correlation was observed between MeHg in the extracellular medium and increased sulfide concentrations (Barrouilhet et al., 2022), indicating that sulfide may facilitate MeHg export and/or enhance desorption from the cell.

3.3 S-containing molecules degradation and production

3.3.1 Sulfide production from Cys degradation by *P. hydrargyri* BerOc1

To control the absence of S-ligands in the medium at t = 0 in the assay, the cells were harvested, washed, and transferred to the experimental medium. When no exogenous Cys was added, sulfide remained undetectable (LOD 20 nM) in the medium for 48 h. Upon introducing exogenous Cys at 0.01, 0.1, and 0.5-mM concentrations, a notable reduction in Cys levels (Figure 4A) and an increase in sulfide production were observed over time (Figure 4B).

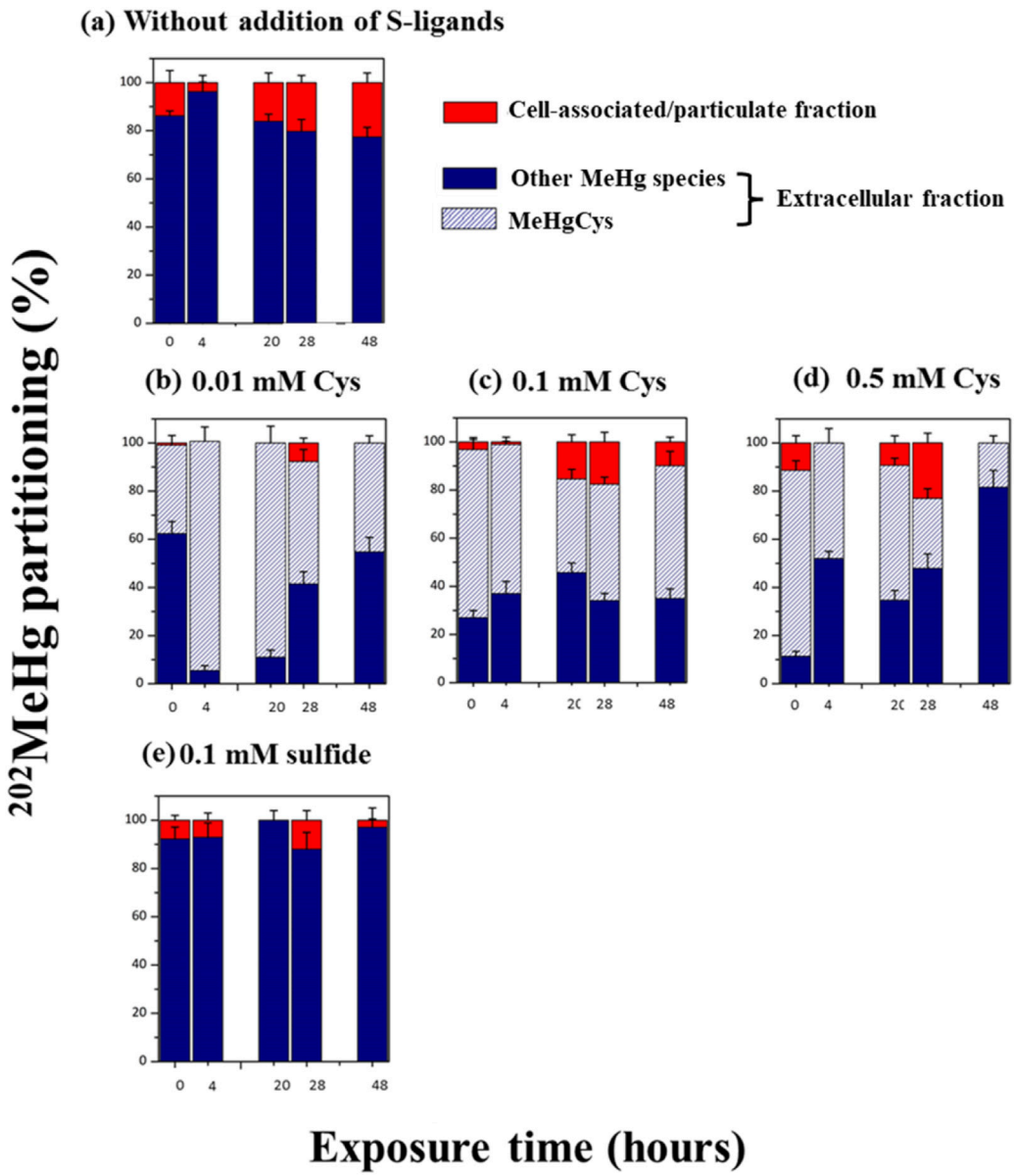

FIGURE 3
Partitioning (%) of added $Me^{202}Hg$ between extracellular (blue), the % of MeHgCys complex detected in the extracellular fraction (blue dash) and cell associated/particulate (red) fractions at the time = 0, 4, 20, 28 and 48 h during exposure to 0.5 μM of $^{199}Hg(II)$ and 0.05 μM of $Me^{202}Hg$. **(a)** Experimental without addition of external S-ligands **(b)** with the addition of 0.01 mM of Cys **(c)** 0.1 mM Cys **(d)** 0.5 mM Cys **(e)** 0.1 mM of sulfide. The percentage was calculated by considering the Hg concentration in the three studied fractions. The same culture batches were used to determine the Hg species in the bulk and extracellular fractions for each kinetics. After sampling for Hg species determination using GCICPMS (bulk + supernatant), cultures were filtered (0.2 μm), and the molecular speciation of MeHg was measured in the extracellular fraction using LCMSMS. Error bars represent the standard deviation of three independent replicates, each measured three times.

After 48 h, the sulfide concentrations in the medium peaked at 4.6 ± 0.2 μM, 42.3 ± 1.9 μM, and 159.3 ± 2.1 μM, corresponding to initial exogenous Cys measurements of 8.2 ± 0.2 μM, 85.5 ± 7.4 μM and 471.4 ± 38.0 μM, respectively (Figures 4A, B). Faster sulfide production and Cys degradation occurred during the first 28 h of exposure, and then the rate decreased, leading to a plateau. Controls with heat-killed cells confirmed that the observed sulfide production from Cys degradation is a fully biotic process, as no sulfide production was observed when heated cells were exposed to 0.1 mM Cys (Figure 4B). Moreover, nanomolar concentration of Cys was detected in the assay without externally added ligands (Figure 4A insert). Increasing Cys concentration led to a higher sulfide concentration in the assay medium; however, the conversion rate of Cys to sulfide did not increase linearly with increasing external Cys (Figure 4C). Previous observations have shown that Cys degradation to sulfide reaches a threshold at 0.5 mM added Cys and above in *E. coli* (Thomas and Gaillard, 2017). Therefore, while increasing the concentration of external Cys may initially increase the conversion rate of Cys to sulfide, there may be a limit to the amount of additional Cys that can be converted, beyond which the

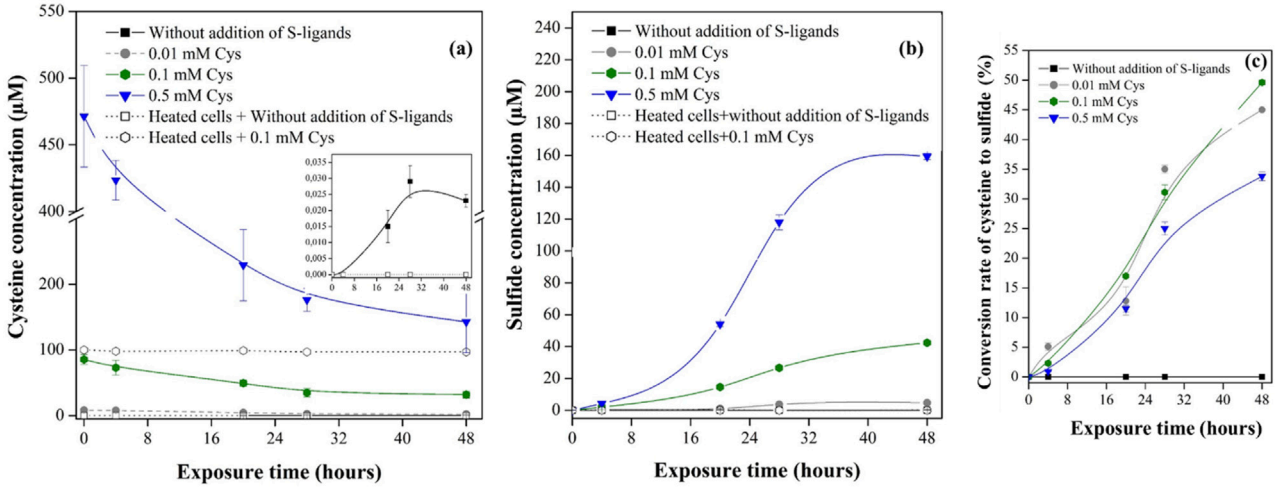

FIGURE 4
(a) Concentration of Cys measured in the extracellular fraction of BerOc1 culture at time = 0, 4, 20, 28 and 48 h during exposure to 0.05 µM of ^{199}Hg(II), 0.05 µM of Me^{202}Hg. The zoom represents the concentrations of Cys detected in the assay without externally added S-ligands. **(b)** Concentration of sulfide in the bulk fraction **(c)** The conversion rate of Cys to sulfide calculated by dividing the sulfide concentration detected at each kinetic point by the initial exogenous Cys concentration. The points are the averages from three independent experiments. Controls were performed with heated cells (80°C for 1 h) exposed to 0.05 µM of ^{199}Hg(II), 0.05 µM of Me^{202}Hg.

conversion rate remains constant or even decreases due to various factors influencing microbial metabolism.

3.3.2 Metabolically active synthesis and cellular export of thiol compounds by *P. hydrargyri* BerOc1

In experiments without the exogenous addition of S-ligands, six different thiol compounds were detected in the extracellular assay medium of metabolically active *P. hydrargyri* BerOc1 (Figure 5A). After 48 h of incubation, the detected LMM-RSH thiols were 2-MPA (35 ± 4 nM), NacCys (30 ± 6 nM), Cys (20 ± 3 nM), HCys (16 ± 2 nM), γ-Glu-Cys (12 ± 3), and Cys-Gly (10 ± 2 nM). The total concentration of thiol compounds reached 123 nM in the assay medium at a cell concentration of 1.1×10^8 cells mL^{-1}. During the first 28 h of incubation, the thiol compounds were rapidly produced and exported (Figure 5A). The assay with heat-killed cells revealed no detectable formation of thiol compounds, indicating that thiols were biosynthesized by BerOc1 via active metabolism and were not produced by dead disrupted cells. The iron-reducer *G. sulfurreducens* PCA has been also shown to produce and export nanomolar concentrations of thiol compounds including Cys, PEN, NacCys, γ-GluCys, Cyst, Glyc, Mac, and HCys (Adediran et al., 2019).

With the addition of exogenous Cys at increasing concentrations, the same thiols were detected in the medium (Figures 5B–D). The total concentration of produced thiol compounds reached 135, 141, and 146 nM for Cys additions of 0.01, 0.1, and 0.5 mM, respectively. The addition of increasing Cys concentration do not impact the production of the other thiols. This suggest that the production of these thiols may be not strongly influenced by changes in Cys levels. Recently, Gutensohn et al., 2023 demonstrated that external exposure of *G. sulfurreducens* PCA to Cys resulted in increased formation of PEN. Experiments using isotopically labeled Cys confirmed that PEN was formed directly from Cys via dimethylation of the C-3 atom. Moreover, PEN was found to not accumulate intracellularly, which could imply that it is part of *G. sulfurreducens* PCA metabolic strategy to maintain Cys homeostasis. In contrast to PCA, PEN was not detected in our experiments with BerOc1. However, BerOc1 degrade Cys and produce sulfide to maintain a low intracellular Cys concentration.

3.4 Implications of cellular thiols metabolism in Hg(II) speciation and bioavailability for methylation

3.4.1 Hg(II) speciation

The addition of exogenous Cys led to sulfide production by *P. hydrargyri* BerOc1. To determine whether Hg(II)-Cys or Hg(II)-sulfide species were favored, we used liquid chromatography-tandem mass spectrometry to measure Hg(Cys)2 formation in the extracellular environment over time. The results, shown as percentages of Hg(Cys)2 relative to total extracellular Hg(II), are displayed in Figure 2. When 0.01 mM Cys was added, about 80% of the introduced ^{199}Hg(II) formed Hg(Cys)2 complexes (Figure 2B). However, with increasing Cys concentrations, the proportion of ^{199}Hg(Cys)2 decreased significantly, reaching 40% and 20% for 0.1 and 0.5 mM Cys, respectively (Figures 2C, D). Chemical modeling predicted HgS(s) formation in all Cys exposure experiments (Supplementary Figure S4). HgS(s) precipitation occurred rapidly, with 100% of Hg(II) forming HgS(s) after 4 h with 0.1 and 0.5 mM Cys, and 20 h with 0.01 mM Cys (Supplementary Figure S4). This indicates that sulfide production from Cys degradation shifted Hg(II) speciation from Hg(Cys)2 to HgS(s), explaining the observed decrease in Hg(Cys)2. Previous research has shown cell-associated HgS(s) formation in *P. hydrargyri* BerOc1 (Isaure et al., 2020) and biomediated HgS(s) formation from Hg(II)-Cys complexes with Cys addition (0.1–1 mM) (Thomas et al., 2018). However, our results do not

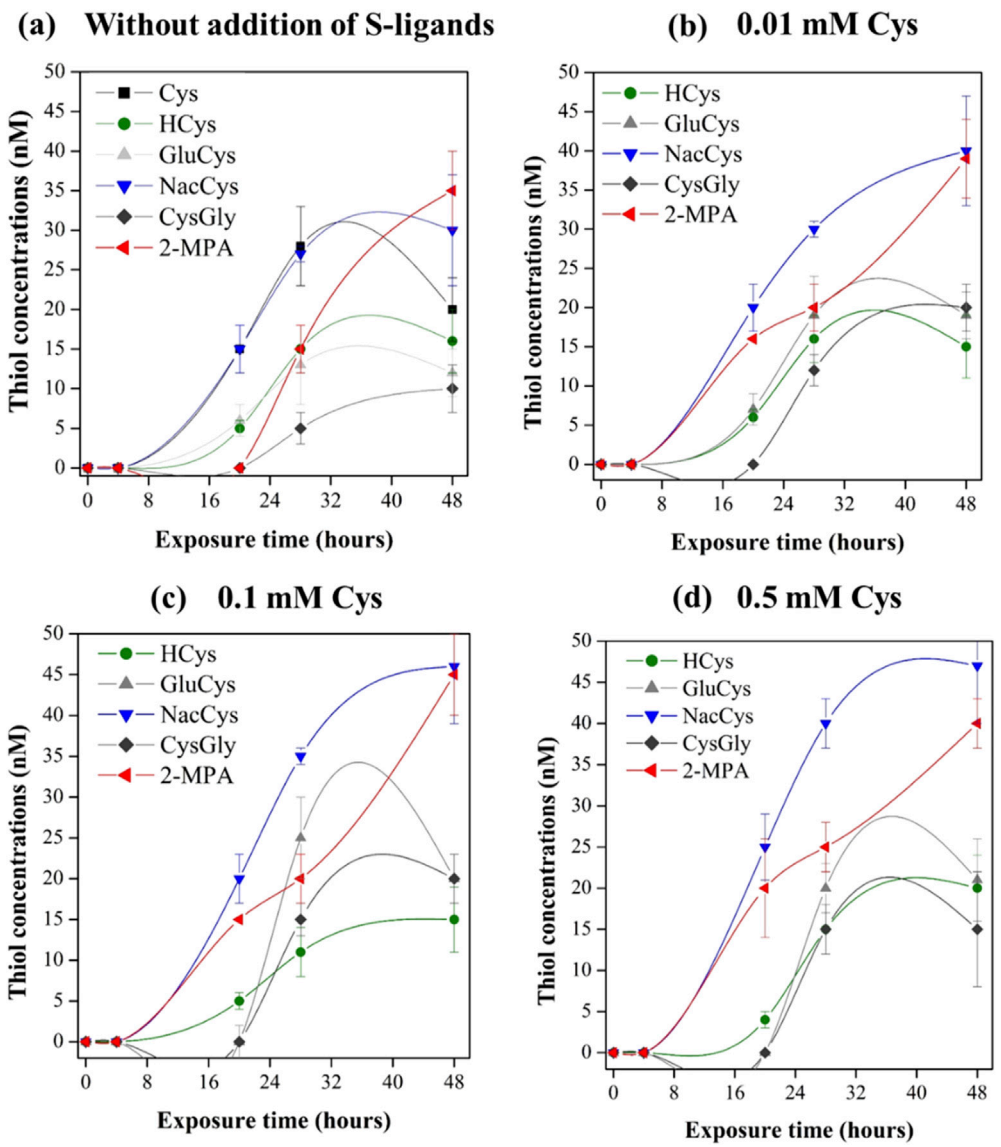

FIGURE 5
Concentrations of biosynthesized LMM-RSH compounds in extracellular assay medium at the time = 0, 4, 20, 28 and 48 h during exposure to 0.5 μM of ^{199}Hg(II) and 0.05 μM of Me^{202}Hg with metabolically active *P. hydrargyri* BerOc1 (~10^8 cells mL-1) for **(a)** Experimental without addition of external S-ligands **(b)** with the addition of 0.01 mM Cys **(c)** 0.1 mM Cys **(d)** 0.5 mM Cys. The thiols detected were Cys, HCys, NacCys, Cys-Gly, γ-Glu-Cys, and 2-MPA. Total biosynthesized thiol concentrations were as follows: **(a)** 123 ± 5 nM, **(b)** 135 ± 6 nM, **(c)** 141 ± 7 nM, and **(d)** 146 ± 5 nM.

fully align with thermodynamic predictions, which suggest 100% Hg(II) as HgS(s) at measured sulfide levels. We detected Hg(Cys) 2 even with sulfide concentrations up to 0.16 mM, indicating the coexistence of Hg(Cys)2 and HgS(s) in the medium.

Without exogenous S-ligands introduction, BerOc1 cells exported six different thiols, including Cys, at nanomolar levels, and ^{199}Hg(Cys)2 (LOD 4 nM) was not detected (Figure 2A). Thermodynamic modeling predicted that $HgCl_2$ (aq), $HgCl_3^-$ (aq), and $HgCl_4^{2-}$ (aq) were the dominant Hg(II) species during the initial incubation hours (Supplementary Figure S4). The metabolically active synthesis and export of thiols by BerOc1 shifted Hg(II) speciation in the medium to HgOH(LMM-RS), HgCl(LMM-RS), and Hg(II)-thiol complexes with a 1: 1 stoichiometry.

3.4.2 Hg(II) bioavailability for methylation

Hg bioavailability for methylation was highest in the absence of externally added S-ligands (only metabolically produced S-ligands were present). Under these conditions, Hg(II) predominantly forms inorganic complexes ($HgOHnCl_{2-n}$) and mixed ligands like HgOH(LMM-RS), HgCl(LMM-RS), and Hg(II)-thiol complexes with 1:1 stoichiometry. This observation suggests that complexes with lower thermodynamic stability can enhance the MeHg formation rate compared to more stable species like $Hg(Cys)_2$ or $HgS_{(s)}$ (Supplementary Table S2). Adediran et al., 2019 (24) determined Hg(II) methylation rate constants for various Hg(II) species in *G. sulfurreducens* PCA, revealing species-specific k′meth values ($\times 10^{-13}$ L cell^{-1} h^{-1}) in the following order: $HgOHnCl_{2-n}$

(k′meth = 45) > HgOHnCl1−n (LMM-RS), Hg (LMM-RORS) (k′meth = 8.8) > $Hg(Cysteamine)_2$ (k′meth = 7.3) > $Hg(Cys)_2$ (k′meth = 3.4) > $Hg(NacCys)_2$ (k′meth = 0.49). These findings imply that Hg(II) complexes with lower thermodynamic stability are more bioavailable for bacterial methylation, reinforcing the notion that the specific nature of metal-ligand interactions plays a crucial role in methylation efficiency. In contrast, previous studies have shown excess Cys (~1–100 μM) promotes Hg(II) uptake and methylation (Schaefer and Morel, 2009; Schaefer et al., 2011; Ndu et al., 2012; Thomas et al., 2014; Szczuka et al., 2015), while nanomolar levels of Cys (<200 nM) decrease Hg(II) methylation (Lu et al., 2016). The increase in Hg(II) methylation with micromolar Cys additions, compared to nanomolar levels, was attributed to a concentration-dependent shift in Hg(II) speciation from HgOHnCl2−n to Hg(Cys)2, presumed to be more bioavailable (Schaefer and Morel, 2009; Lin et al., 2015). However, Adediran et al., 2019 found that in the iron-reducing *G. sulfurreducens* PCA, the enhancement in Hg(II) methylation with micromolar Cys (0–10 μM) was not solely due to changes in Hg(II) speciation, suggesting that other biochemical pathways regulating Hg(II) methylation warrant further investigation.

Our results align with the framework that indicates as the thermodynamic stability of an aqueous metal complex increases, the bioavailability of the metal decreases (Morel et al., 1991; Slaveykova et al., 2005; Xu et al., 2012). We observed a higher Kmeth for less stable Hg(II) complexes, underscoring that biotic ligand models explain much of the data, yet some aspects of Hg(II) uptake and methylation remain inadequately addressed by ligand affinity alone. This is crucial, as less stable mixed ligand Hg(II) species, while not predominant in thermodynamic equilibrium, may be kinetically favored under specific conditions (Miller et al., 2009; Jiang et al., 2015), Our study demonstrates that these species can significantly contribute to MeHg formation when present.

The mechanisms of Hg(II) uptake by methylating microorganisms remain to be fully elucidated. Proposed mechanisms include the uptake of thermodynamically stable Hg(II) species via passive diffusion of neutral HgS^0(aq) and $Hg(SH)_2^0$ (aq) (Benoit et al., 1999), and active uptake processes for the $Hg(Cys)_2$ complex (Schaefer and Morel, 2009). Additionally, metal uptake likely involves binding to cell surface functional groups (Hudson, 1998; Campbell et al., 2002), with mechanisms such as ligand exchange reactions, either through complex dissociation in solution (Slaveykova et al., 2005; Di Toro et al., 2001) or transient ternary complex formation (Aristilde et al., 2012; Flynn et al., 2014; Fein, 2017). Regardless of the uptake mechanism, the metal transfer rate from solution to cell surface depends on the metal's affinity for aqueous and cell surface ligands and their relative concentration (Zhao et al., 2016). As the thermodynamic stability of an aqueous metal complex increases, the bioavailability of the metal decreases (Morel et al., 1991; Slaveykova et al., 2005; Xu et al., 2012). Our results, showing a higher Kmeth for less stable Hg(II) complexes, align with this framework. Although biotic ligand models explain most data, some aspects of Hg(II) uptake and methylation remain unexplained by ligand affinity alone.

3.5 Implications of cellular thiols metabolism in MeHg speciation and bioavailability for demethylation

The formation of MeHg-Cys in the extracellular medium was quantified using liquid chromatography tandem mass spectrometry. Figure 3 displays the percentage of $Me^{202}Hg$-Cys species relative to total extracellular $Me^{202}Hg$. The experiments involving Cys addition demonstrated that $Me^{202}Hg$ formed complexes with Cys to produce $Me^{202}Hg$-Cys (Figure 3). The proportion of $Me^{202}Hg$-Cys in the extracellular medium remained relatively stable (approximately 60%–80% of total added $Me^{202}Hg$) as Cys concentrations increased from 0.01 to 0.1 mM. However, at the highest Cys exposure (0.5 mM), the concentration of $Me^{202}HgCys$ significantly decreased over time, reaching only 10% of the added $Me^{202}Hg$ after 48 h (Figure 3). To investigate the formation of MeHg-sulfide species under the experimental conditions, thermodynamic modeling was conducted. Chemical modeling of MeHg revealed the presence of MeHgSH and S (MeHg)2 in all experiments with Cys exposure (Supplementary Figure S5). The formation of MeHgSH increased with higher Cys concentrations, reaching 100% of MeHg at 0.5 mM addition. This explains the observed decrease in $Me^{202}HgCys$, which can be attributed to a shift in MeHg chemical speciation from MeHgCys to MeHgSH and S (MeHg)2. In experiments without externally added S-ligands, $MeHg^{202}Cys$ was not detected. Thermodynamic modeling was performed to examine the species formed in the absence of excess S ligands (Supplementary Figure S5). MeHgCl was found to be the dominant MeHg species throughout the exposure period. The metabolically active synthesis and cellular export of thiol compounds (LMM-RSH) by *P. hydrargyri* BerOc1 did not alter the chemical speciation of MeHg in the assay media. While extensive literature exists on the thermodynamics of Hg(II) complexation (Dyrssen and Wedborg, 1991; Ravichandran, 2004; Smith et al., 2004; Cardiano et al., 2011; Drott et al., 2013; Warner and Jalilehvand, 2016; Liem-Nguyen et al., 2017b), there is less data available on the thermodynamic formation constant for MeHg, particularly regarding its complexation with thiol compounds. This lack of data may lead to an underestimation of MeHg-thiol compound formation. This study demonstrated that the addition of S-ligands (Cys and sulfide) induced a change in the chemical speciation of MeHg. However, the shift in MeHg chemical speciation from MeHgCl to MeHgCys, MeHgSH, and S (MeHg)2 did not impact demethylation rates (Kdemeth).

4 Conclusion

In this work, Hg(II) and MeHg speciation and molecular transformations were investigated using the model strain *P. hydrargyri* BerOc1. The use of isotopic enriched mercury species allowed precise tracking of mercury species and their transformations. We showed that the highest methylation rate (K_{meth}) was obtained under conditions without addition of ligands. Under such conditions, by quantifying and taking in account microbial produced thiols, refined speciation models were generated. These models revealed that Hg(II) formed complexes with mixed binding involving biosynthesized thiols, OH^- ions and Cl^- ions. Our results suggest that these complexes

increase the rate of MeHg formation compared to the more stable $Hg(Cys)_2$ or $HgS_{(s)}$ species. Unlike Hg(II) methylation, the addition of S-ligands did not affect the rates of demethylation of MeHg, even though it caused a shift in the chemical speciation of MeHg. The results of this study provide valuable insights into the underlying mechanisms of mercury methylation and demethylation.

Data availability statement

The original contributions presented in the study are included in the article/Supplementary Material, further inquiries can be directed to the corresponding author.

Author contributions

IK: Conceptualization, Data curation, Formal analysis, Validation, Vizualization, Writing–original draft, Writing–review and editing. M-PI: Conceptualization, Validation, Vizualization, Writing–original draft, Writing–review and editing, Supervision, Funding acquisition, SB: Conceptualization, Data curation, Formal analysis, Writing-review and editing. MS-G: Conceptualization, Validation, Vizualization, Writing–original draft, Writing–review and editing, Supervision, Funding acquisition. MM: Conceptualization, Data curation, Formal analysis, Validation, Vizualization, Writing–original draft, Writing–review and editing, Supervision, Funding acquisition

Funding

The author(s) declare that financial support was received for the research, authorship, and/or publication of this article. This work was supported by the Go-Beam project, funded by the Agence Nationale de la Recherche, through the E2S-UPPA call Key Scientific challenges.

Conflict of interest

The authors declare that the research was conducted in the absence of any commercial or financial relationships that could be construed as a potential conflict of interest.

Generative AI statement

The author(s) declare that no Generative AI was used in the creation of this manuscript.

Publisher's note

All claims expressed in this article are solely those of the authors and do not necessarily represent those of their affiliated organizations, or those of the publisher, the editors and the reviewers. Any product that may be evaluated in this article, or claim that may be made by its manufacturer, is not guaranteed or endorsed by the publisher.

Supplementary material

The Supplementary Material for this article can be found online at: https://www.frontiersin.org/articles/10.3389/fenvc.2025.1559968/full#supplementary-material

References

Adediran, G. A., Liem-Nguyen, V., Song, Y., Schaefer, J. K., Skyllberg, U., and Björn, E. (2019). Microbial biosynthesis of thiol compounds: implications for speciation, cellular uptake, and methylation of Hg(II). *Environ. Sci. Technol.* 53 (14), 8187–8196. doi:10.1021/acs.est.9b01502

Aristilde, L., Xu, Y., and Morel, F. M. M. (2012). Weak organic ligands enhance zinc uptake in marine phytoplankton. *Environ. Sci. Technol.* 46 (10), 5438–5445. doi:10.1021/es300335u

Awano, N., Wada, M., Mori, H., Nakamori, S., and Takagi, H. (2005). Identification and functional analysis of *Escherichia coli* cysteine desulfhydrases. *Appl. Environ. Microbiol.* 71 (7), 4149–4152. doi:10.1128/aem.71.7.4149-4152.2005

Bakour, I., Isaure, M. P., Barrouilhet, S., Goñi-Urriza, M., and Monperrus, M. (2023). Coupling fluorescent probes to characterize S-containing compounds in a sulfate reducing bacteria involved in Hg methylation. *Talanta Open* 7, 100228. doi:10.1016/j.talo.2023.100228

Barrouilhet, S., Monperrus, M., Tessier, E., Khalfaoui-Hassani, B., Guyoneaud, R., Isaure, M. P., et al. (2022). Effect of exogenous and endogenous sulfide on the production and the export of methylmercury by sulfate-reducing bacteria. *Environ. Sci. Pollut. Res.* 30, 3835–3846. doi:10.1007/s11356-022-22173-y

Benoit, J. M., Gilmour, C. C., Mason, R. P., and Heyes, A. (1999). Sulfide controls on mercury speciation and bioavailability to methylating bacteria in sediment pore waters. *Environ. Sci. Technol.* 33 (6), 951–957. doi:10.1021/es9808200

Bravo, A. G., Zopfi, J., Buck, M., Xu, J., Bertilsson, S., Schaefer, J. K., et al. (2018). Geobacteraceae are important members of mercury-methylating microbial communities of sediments impacted by waste water releases. *ISME J.* 12 (3), 802–812. doi:10.1038/s41396-017-0007-7

Bridou, R., Monperrus, M., Gonzalez, P. R., Guyoneaud, R., and Amouroux, D. (2011). Simultaneous determination of mercury methylation and demethylation capacities of various sulfate-reducing bacteria using species-specific isotopic tracers. *Environ. Toxicol. Chem.* 30 (2), 337–344. doi:10.1002/etc.395

Campbell, P. G. C., Errécalde, O., Fortin, C., Hiriart-Baer, V. P., and Vigneault, B. (2002). Metal bioavailability to phytoplankton—applicability of the biotic ligand model. *Comp. Biochem. Physiology Part C Toxicol. and Pharmacol.* 133 (1), 189–206. doi:10.1016/s1532-0456(02)00104-7

Cardiano, P., Falcone, G., Foti, C., and Sammartano, S. (2011). Sequestration of Hg2+ by some biologically important thiols. *J. Chem. and Eng. Data*, 56. doi:10.1021/je200735r

Compeau, G. C., and Bartha, R. (1985). Sulfate-reducing bacteria: principal methylators of mercury in anoxic estuarine sediment. *Appl. Environ. Microbiol.* 50 (2), 498–502. doi:10.1128/aem.50.2.498-502.1985

Deonarine, A., and Hsu-Kim, H. (2009). Precipitation of mercuric sulfide nanoparticles in NOM-containing water: implications for the natural environment. *Environ. Sci. Technol.* 43 (7), 2368–2373. doi:10.1021/es803130h

Di Toro, D. M., Allen, H. E., Bergman, H. L., Meyer, J. S., Paquin, P. R., and Santore, R. C. (2001). Biotic ligand model of the acute toxicity of metals. 1. Technical basis. *Environ. Toxicol. Chem.* 20 (10), 2383–2396. doi:10.1897/1551-5028(2001)020<2383:blmota>2.0.co;2

Drott, A., Björn, E., Bouchet, S., and Skyllberg, U. (2013). Refining thermodynamic constants for mercury(II)-Sulfides in equilibrium with metacinnabar at sub-micromolar aqueous sulfide concentrations. *Environ. Sci. Technol.* 47 (9), 4197–4203. doi:10.1021/es304824n

Dyrssen, D., and Wedborg, M. (1991). The sulphur-mercury(II) system in natural waters. *Water, Air, Soil Pollut.* 56 (1), 507–519. doi:10.1007/bf00342295

Fein, J. B. (2017). Advanced biotic ligand models: using surface complexation modeling to quantify metal bioavailability to bacteria in geologic systems. *Chem. Geol.* 464, 127–136. doi:10.1016/j.chemgeo.2016.10.001

Flynn, S. L., Szymanowski, J. E. S., and Fein, J. B. (2014). Modeling bacterial metal toxicity using a surface complexation approach. *Chem. Geol.* 374–375, 110–116. doi:10.1016/j.chemgeo.2014.03.010

Gerbig, C., Kim, C., Stegemeier, J., Ryan, J., and Aiken, G. (2011). Formation of nanocolloidal metacinnabar in mercury-DOM-sulfide systems. *Environ. Sci. and Technol.* 45, 9180–9187. doi:10.1021/es201837h

Gilmour, C. C., Bullock, A. L., McBurney, A., Podar, M., and Elias, D. A. (2018). Robust mercury methylation across diverse methanogenic *archaea*. Lovley DR. *mBio* 9 (2), e02403. doi:10.1128/mBio.02403-17

Gilmour, C. C., Elias, D. A., Kucken, A. M., Brown, S. D., Palumbo, A. V., Schadt, C. W., et al. (2011). Sulfate-reducing bacterium Desulfovibrio desulfuricans ND132 as a model for understanding bacterial mercury methylation. *Appl. Environ. Microbiol.* 77 (12), 3938–3951. doi:10.1128/aem.02993-10

Gilmour, C. C., Podar, M., Bullock, A. L., Graham, A. M., Brown, S. D., Somenahally, A. C., et al. (2013). Mercury methylation by novel microorganisms from new environments. *Environ. Sci. Technol.* 47 (20), 11810–11820. doi:10.1021/es403075t

Goñi-Urriza, M., Corsellis, Y., Lanceleur, L., Tessier, E., Gury, J., Monperrus, M., et al. (2015). Relationships between bacterial energetic metabolism, mercury methylation potential, and hgcA/hgcB gene expression in Desulfovibrio dechloroacetivorans BerOc1. *Environ. Sci. Pollut. Res. Int.* 22 (18), 13764–13771. doi:10.1007/s11356-015-4273-5

Goñi-Urriza, M., Klopp, C., Ranchou-Peyruse, M., Ranchou-Peyruse, A., Monperrus, M., Khalfaoui-Hassani, B., et al. (2020). Genome insights of mercury methylation among Desulfovibrio and Pseudodesulfovibrio strains. *Res. Microbiol.* 171 (1), 3–12. doi:10.1016/j.resmic.2019.10.003

Graham, A. M., Aiken, G. R., and Gilmour, C. C. (2012b). Dissolved organic matter enhances microbial mercury methylation under sulfidic conditions. *Environ. Sci. Technol.* 46 (5), 2715–2723. doi:10.1021/es203658f

Graham, A. M., Aiken, G. R., and Gilmour, C. C. (2013). Effect of dissolved organic matter source and character on microbial Hg methylation in Hg–S–dom solutions. *Environ. Sci. Technol.* 47 (11), 5746–5754. doi:10.1021/es400414a

Graham, A. M., Bullock, A. L., Maizel, A. C., Elias, D. A., and Gilmour, C. C. (2012a). Detailed assessment of the kinetics of Hg-cell association, Hg methylation, and methylmercury degradation in several Desulfovibrio species. *Appl. Environ. Microbiol.* 78 (20), 7337–7346. doi:10.1128/aem.01792-12

Gutensohn, M., Schaefer, J. K., Maas, T. J., Skyllberg, U., and Björn, E. (2023). Metabolic turnover of cysteine-related thiol compounds at environmentally relevant concentrations by Geobacter sulfurreducens. *Front. Microbiol.* 13, 1085214. doi:10.3389/fmicb.2022.1085214

Hand, C. E., and Honek, J. F. (2005). Biological chemistry of naturally occurring thiols of microbial and marine Origin. *J. Nat. Prod.* 68 (2), 293–308. doi:10.1021/np049685x

Hudson, R. J. M. (1998). Which aqueous species control the rates of trace metal uptake by aquatic biota? Observations and predictions of non-equilibrium effects. *Sci. Total Environ.* 219 (2), 95–115. doi:10.1016/s0048-9697(98)00230-7

Isaure, M. P., Albertelli, M., Kieffer, I., Tucoulou, R., Petrel, M., Gontier, E., et al. (2020). Relationship between Hg speciation and Hg methylation/demethylation processes in the sulfate-reducing bacterium Pseudodesulfovibrio hydrargyri: evidences from HERFD-XANES and nano-XRF. *Front. Microbiol.* 11, 584715. doi:10.3389/fmicb.2020.584715

Jiang, T., Skyllberg, U., Wei, S., Wang, D., Lu, S., Jiang, Z., et al. (2015). Modeling of the structure-specific kinetics of abiotic, dark reduction of Hg(II) complexed by O/N and S functional groups in humic acids while accounting for time-dependent structural rearrangement. *Geochimica Cosmochimica Acta* 154, 151–167. doi:10.1016/j.gca.2015.01.011

Liem-Nguyen, V., Bouchet, S., and Björn, E. (2015). Determination of sub-nanomolar levels of low molecular mass thiols in natural waters by liquid chromatography tandem mass spectrometry after derivatization with p-(hydroxymercuri) benzoate and online preconcentration. *Anal. Chem.* 87 (2), 1089–1096. doi:10.1021/ac503679y

Liem-Nguyen, V., Nguyen-Ngoc, H. T., Adediran, G. A., and Björn, E. (2020). Determination of picomolar levels of methylmercury complexes with low molecular mass thiols by liquid chromatography tandem mass spectrometry and online preconcentration. *Anal. Bioanal. Chem.* 412 (7), 1619–1628. doi:10.1007/s00216-020-02389-y

Liem-Nguyen, V., Skyllberg, U., and Björn, E. (2017a). Thermodynamic modeling of the solubility and chemical speciation of mercury and methylmercury driven by organic thiols and micromolar sulfide concentrations in boreal wetland soils. *Environ. Sci. Technol.* 51 (7), 3678–3686. doi:10.1021/acs.est.6b04622

Liem-Nguyen, V., Skyllberg, U., Nam, K., Björn, E., Liem-Nguyen, V., Skyllberg, U., et al. (2017b). Thermodynamic stability of mercury(II) complexes formed with environmentally relevant low-molecular-mass thiols studied by competing ligand exchange and density functional theory. *Environ. Chem.* 14 (4), 243–253. doi:10.1071/en17062

Lin, H., Lu, X., Liang, L., and Gu, B. (2015). Cysteine inhibits mercury methylation by *Geobacter sulfurreducens* PCA mutant Δ *omcBESTZ*. *Environ. Sci. and Technol. Lett.* 2 (5), 144–148. doi:10.1021/acs.estlett.5b00068

Lu, X., Liu, Y., Johs, A., Zhao, L., Wang, T., Yang, Z., et al. (2016). Anaerobic mercury methylation and demethylation by *Geobacter bemidjiensis* bem. *Environ. Sci. and Technol.* 50 (8), 4366–4373. doi:10.1021/acs.est.6b00401

Miller, C. L., Southworth, G., Brooks, S., Liang, L., and Gu, B. (2009). Kinetic controls on the complexation between mercury and dissolved organic matter in a contaminated environment. *Environ. Sci. Technol.* 43 (22), 8548–8553. doi:10.1021/es901891t

Morel, F. M. M., Hudson, R. J. M., and Price, N. M. (1991). Limitation of productivity by trace metals in the sea. *Limnol. Oceanogr.* 36 (8), 1742–1755. doi:10.4319/lo.1991.36.8.1742

Ndu, U., Mason, R. P., Zhang, H., Lin, S., and Visscher, P. T. (2012). Effect of inorganic and organic ligands on the bioavailability of methylmercury as determined by using a mer-lux bioreporter. *Appl. Environ. Microbiol.* 78 (20), 7276–7282. doi:10.1128/aem.00362-12

Parks, J. M., Johs, A., Podar, M., Bridou, R., Hurt, R. A., Smith, S. D., et al. (2013). The genetic basis for bacterial mercury methylation. *Science.* 339 (6125), 1332–1335. doi:10.1126/science.1230667

Pedrero, Z., Bridou, R., Mounicou, S., Guyoneaud, R., Monperrus, M., and Amouroux, D. (2012). Transformation, localization, and biomolecular binding of Hg species at subcellular level in methylating and nonmethylating sulfate-reducing bacteria. *Environ. Sci. Technol.* 46 (21), 11744–11751. doi:10.1021/es302412q

Perrot, V., Bridou, R., Pedrero, Z., Guyoneaud, R., Monperrus, M., and Amouroux, D. (2015). Identical Hg isotope mass dependent fractionation signature during methylation by sulfate-reducing bacteria in sulfate and sulfate-free environment. *Environ. Sci. Technol.* 49 (3), 1365–1373. doi:10.1021/es5033376

Pham, A. L. T., Morris, A., Zhang, T., Ticknor, J., Levard, C., and Hsu-Kim, H. (2014). Precipitation of nanoscale mercuric sulfides in the presence of natural organic matter: structural properties, aggregation, and biotransformation. *Geochimica Cosmochimica Acta* 133, 204–215. doi:10.1016/j.gca.2014.02.027

Ranchou-Peyruse, M., Monperrus, M., Bridou, R., Duran, R., Amouroux, D., Salvado, J. C., et al. (2009). Overview of mercury methylation capacities among anaerobic bacteria including representatives of the sulphate-reducers: implications for environmental studies. *Geomicrobiol. J.* 26 (1), 1–8. doi:10.1080/01490450802599227

Ravichandran, M. (2004). Interactions between mercury and dissolved organic matter–a review. *Chemosphere* 55 (3), 319–331. doi:10.1016/j.chemosphere.2003.11.011

Rodríguez-González, P., Monperrus, M., Alonso, J. I. G., Amouroux, D., and Donard Of, X. (2007). Comparison of different numerical approaches for multiple spiking species-specific isotope dilution analysis exemplified by the determination of butyltin species in sediments. *J. Anal. Atomic Spectrom.* 22 (11), 1373–1382. doi:10.1039/b706542f

Rodrı´guez Martı´n-Doimeadios, R. C., Tessier, E., Amouroux, D., Guyoneaud, R., Duran, R., Caumette, P., et al. (2004). Mercury methylation/demethylation and volatilization pathways in estuarine sediment slurries using species-specific enriched stable isotopes. *Mar. Chem.* 90 (1), 107–123. doi:10.1016/j.marchem.2004.02.022

Schaefer, J. K., and Morel, F. M. M. (2009). High methylation rates of mercury bound to cysteine by Geobacter sulfurreducens. *Nat. Geosci.* 2 (2), 123–126. doi:10.1038/ngeo412

Schaefer, J. K., Rocks, S. S., Zheng, W., Liang, L., Gu, B., and Morel, F. M. M. (2011). Active transport, substrate specificity, and methylation of Hg(II) in anaerobic bacteria. *PNAS* 108 (21), 8714–8719. doi:10.1073/pnas.1105781108

Shimada, T., Tanaka, K., and Ishihama, A. (2016). Transcription factor DecR (YbaO) controls detoxification of L-cysteine in *Escherichia coli*. *Microbiol. Read.* 162 (9), 1698–1707. doi:10.1099/mic.0.000337

Slaveykova, V. I., Wilkinson, K. J., Slaveykova, V. I., and Wilkinson, K. J. (2005). Predicting the bioavailability of metals and metal complexes: critical review of the biotic ligand model. *Environ. Chem.* 2 (1), 9–24. doi:10.1071/en04076

Smith, R. M., Martell, A., Motekaitis, R., Smith, R., and Motekaitis, R. (2004). NIST critically selected stability constants of metal complexes database. Available online at: https://www.semanticscholar.org/paper/NIST-Critically-Selected-Stability-Constants-of-Smith-Martell/4d1e936ecb2cd7c641ada4f9db589ad5b50072ba.

Stenzler, B. R., Zhang, R., Semrau, J. D., DiSpirito, A. A., and Poulain, A. J. (2022). Diffusion of H_2S from anaerobic thiolated ligand biodegradation rapidly generates bioavailable mercury. *Environ. Microbiol.* 24 (7), 3212–3228. doi:10.1111/1462-2920.16078

Szczuka, A., Morel, F. M. M., and Schaefer, J. K. (2015). Effect of thiols, zinc, and redox conditions on Hg uptake in shewanella oneidensis. *Environ. Sci. Technol.* 49 (12), 7432–7438. doi:10.1021/acs.est.5b00676

Thomas, S. A., Catty, P., Hazemann, J. L., Michaud-Soret, I., and Gaillard, J. F. (2019). The role of cysteine and sulfide in the interplay between microbial Hg(II) uptake and sulfur metabolism. *Metallomics.* 11 (7), 1219–1229. doi:10.1039/c9mt00077a

Thomas, S. A., and Gaillard, J. F. (2017). Cysteine addition promotes sulfide production and 4-fold Hg(II)–S coordination in actively metabolizing *Escherichia coli*. *Environ. Sci. Technol.* 51 (8), 4642–4651. doi:10.1021/acs.est.6b06400

Thomas, S. A., Rodby, K. E., Roth, E. W., Wu, J., and Gaillard, J. F. (2018). Spectroscopic and microscopic evidence of biomediated HgS species formation from Hg(II)–Cysteine complexes: implications for Hg(II) bioavailability. *Environ. Sci. Technol.* 52 (17), 10030–10039. doi:10.1021/acs.est.8b01305

Thomas, S. A., Tong, T., and Gaillard, J. F. (2014). Hg(ii) bacterial biouptake: the role of anthropogenic and biogenic ligands present in solution and spectroscopic evidence of ligand exchange reactions at the cell surface. *Metallomics* 6 (12), 2213–2222. doi:10.1039/c4mt00172a

Warner, T., and Jalilehvand, F. (2016). Formation of Hg(II) tetrathiolate complexes with cysteine at neutral pH. *Can. J. Chem.* 94 (4), 373–379. doi:10.1139/cjc-2015-0375

Widdel, F., and Bak, F. (1992). "Gram-negative mesophilic sulfate-reducing bacteria," in *The prokaryotes: a handbook on the biology of bacteria: ecophysiology, isolation, identification, applications*. Editors A. Balows, H. G. Trüper, M. Dworkin, W. Harder, and K. H. Schleifer (New York, NY: Springer), 3352–3378. doi:10.1007/978-1-4757-2191-1_21

Xu, Y., Shi, D., Aristilde, L., and Morel, F. M. M. (2012). The effect of pH on the uptake of zinc and cadmium in marine phytoplankton: possible role of weak complexes. *Limnol. Oceanogr.* 57 (1), 293–304. doi:10.4319/lo.2012.57.1.0293

Yang, Y., Feng, Y., Jiang, Y., Qiu, F., Wang, Y., Song, X., et al. (2019). A coumarin-based colorimetric fluorescent probe for rapid response and highly sensitive detection of hydrogen sulfide in living cells. *Talanta* 197, 122–129. doi:10.1016/j.talanta.2018.12.081

Zhang, T., Kim, B., Levard, C., Reinsch, B. C., Lowry, G. V., Deshusses, M. A., et al. (2012). Methylation of mercury by bacteria exposed to dissolved, nanoparticulate, and microparticulate mercuric sulfides. *Environ. Sci. Technol.* 46 (13), 6950–6958. doi:10.1021/es203181m

Zhao, C. M., Campbell, P. G. C., and Wilkinson, K. J. (2016). When are metal complexes bioavailable? *Environ. Chem.* 13 (3), 425. doi:10.1071/en15205